Materials Research. 2016; 19(2): 413-419
DOI:http://dx.doi.org/10.1590/1980-5373-MR-2015-0411

Investigations on the Synthesis, Optical and Electrical Properties of TiO_2 Thin Films by Chemical Bath Deposition (CBD) method

Geetha Govindasamy[a], Priya Murugasen[b], Suresh Sagadevan[c]*

[a]Bharathiar University, Coimbatore, India
[b]Department of Physics, Saveetha Engineering College, Chennai, 600 123, India
[c]Department of Physics, AMET University, Chennai, 603 112, India

Received: July 16, 2015; Revised: November 19, 2015; Accepted: January 4, 2016

Titanium dioxide (TiO_2) thin films were prepared by Chemical Bath Deposition (CBD) method. The X-ray diffraction (XRD) analysis was used to examine the structure and to determine the crystallite size of TiO_2 thin film. The surface morphology of the film was studied using Scanning Electron Microscopy (SEM).The optical properties were studied using the UV-Visible and photoluminescence (PL) spectrum. Optical constants such as band gap, refractive index, extinction coefficient and electric susceptibility were determined. The FT-IR spectrum revealed the strong presence of TiO_2. The dielectric properties of TiO_2 thin films were studied for different frequencies and different temperatures. The AC electrical conductivity test revealed that the conduction depended both on the frequency and the temperature. Photoconductivity study was carried out in order to ascertain the positive photoconductivity of the TiO_2 thin films.

Keywords: *TiO_2 thin films, XRD, SEM analysis, Photoluminescence (PL), FTIR, Dielectric constant and Dielectric loss*

1. INTRODUCTION

The study of semiconducting thin films is being pursued with growing interest on account of their established and useful applications in many semiconductor devices such as solar energy converters, optoelectronics devices etc [1]. In the recent decades, there has been an enormous deal of attention being bestowed upon the making of inexpensive thin films, due to their high varying characteristics. Such characteristics consist of high resistivity, heat reflecting windows, catalytic properties, photo thermal and photovoltaic [2] . Titanium dioxide (TiO_2) is an extensively used material for optical and protective applications because of its high transparency in the visible region, excellent mechanical durability and chemical stability in aqueous solution [3,4]. TiO_2 films are valuable for such applications as catalysis, optical coatings, gas sensors, and other electronic devices [5-7]. The physical and chemical properties of TiO_2 are such that it becomes suitable for a wide spectrum of applications. It is also an excellent electrode material that can be used for the conversion of light energy into electrical energy because of its semiconductor properties. Its wide applications such as supercapacitors, dye-sensitized solar cells, quantum-dot-sensitized solar cells, lithium ion batteries, photoelectrolysis, water splitting, biosensors, photochromic devices, self-cleaning, and extremely thin absorber (ETA) solar cells have already been explored [8-17] . TiO_2 films can be synthesized by many chemical and physical deposition techniques, such as chemical vapor deposition, spin coating or spin casting, atomic layer deposition, molecular beam epitaxy, sputtering, cathodic arc deposition, electrospray deposition, sol–gel process [18]. It has been established by research that the preparation technique and processing conditions strongly impact the microstructure and physical properties of the material. Each technique has its own advantages and limitations. The CBD method has almost become the favourite of many researchers who see it as a comfortable alternative technique for the synthesis of metal chalcogenide thin films because of its advantages such as low cost and large-area deposition. CBD technique facilitates the formation of thin films of metal chalcogenides by spontaneous reaction in solution. TiO_2 thin films have also been prepared by sol-gel chemical bath deposition technique [19]. CBD technique has several advantages over the other ones. For instance, this method can be used for large area deposition at room temperature and the thickness of the deposited layer can be readily controlled by varying the length of the deposition time. Earlier investigations of the microstructural and optical properties of TiO_2 films synthesized by the CBD technique had shed much light. They have shown that the characteristics such as film thickness, bonding configuration, optical absorption and optical bandgap and structure are a function of deposition time [20]. Based on this fact we report the synthesis and the characterization of TiO_2 thin films. The prepared films were characterized for their structural, surface morphology, optical properties, photoluminescence, FTIR analysis, and electrical studies. The results of the characterization studies are discussed in the paper.

*e-mail: drsureshphysics@gmail.com

2. EXPERIMENTAL PROCEDURE

The TiO_2 thin films were deposited by means of CBD technique at room temperature using titanium tetra isopropoxide and isopropanol as the starting materials. For thin film deposition the starting materials of 5 ml titanium tetra isopropoxide ($Ti\{OCH(CH_3)_2\}_4$) and 10 ml isoproponal (C_3H_8O) were dissolved in 100 ml of distilled water in a glass vessel. The vessel with reactive solution was kept in the room temperature. Glacial acetic acid ($C_2H_4O_2$) was added drop by drop to the solution. The solution was stirred well with the help of a magnetic stirrer to maintain the homogeneous mixture. The deposition was carried out at the temperature of 80°C and the growth time was 3 h. A glass substrate was placed vertically inside the vessel with the help of a suitably designed substrate holder. After three hours, the glass slide was removed from the bath and cleaned with deionized water and dried in a hot oven. The resultant films were homogeneous and well adhered to the substrate with mirror like surface.

3. CHARACTERIZATION TECHNIQUES

The X-ray diffraction analysis (XRD) pattern of the TiO_2 thin films was recorded by using a powder X-ray diffractometer (Schimadzu model: XRD 6000 using CuKα (λ=0.154 nm)) radiation, with a diffraction angle between 10° and 70°. The crystallite size was determined from the broadenings of corresponding X-ray spectrum peaks by using Scherrer's formula. Scanning Electron Microscopy (SEM) studies were carried out on JEOL, JSM- 67001. The optical absorption spectrum of the TiO_2 thin films was taken by using the VARIAN CARY MODEL 5000 spectrophotometer in the wavelength range of 300 – 800 nm. The PL spectrum of the TiO_2 thin films was recorded by using the Perkin-Elmer lambda 900 spectrophotometer with a Xe lamp as the excitation light source. The FTIR spectrum of the TiO_2 thin films was taken using an FTIR model Bruker IFS 66W Spectrometer. The dielectric properties of the TiO_2 thin films were analyzed using a HIOKI 3532-50 LCR HITESTER over the frequency range 50Hz-5MHz. Photoconductivity measurements were carried out at room temperature by connecting the sample prepared in series with a picoammeter (Keithley 480) and a dc power supply.

4. RESULTS AND DISCUSSION

4.1 Structural studies

The phase composition and the structure of the film were studied by X-ray diffraction analysis. The XRD patterns of TiO_2 thin films are shown in Fig.1. The strong and sharp diffraction peaks indicate the formation of well crystallized TiO_2 thin films. The diffraction pattern shows a peak (101) plane of the anatase phase of TiO_2. The observed peaks correspond to (1 0 1), (0 0 4), (2 0 0), (1 0 5), and (2 0 4) planes. No peaks corresponding to the rutile or brookite phase were observed in the X-ray diffraction pattern. The average nano-crystalline size (D) was calculated using the Scherrer formula,

$$D = \frac{0.9\lambda}{\beta \cos\theta} \quad (1)$$

where λ is the X-ray wavelength (CuKα radiation and equals to 0.154 nm), θ is the Bragg diffraction angle, and β is the full width half maximum (FWHM) of the XRD peak appearing at the diffraction angle θ. The average crystalline size was calculated from the X-ray line broadening peak and Scherrer equation and it was found to be about 18 nm.

4.2 SEM analysis

Scanning electron microscopy (SEM) was employed for the investigation of morphological features of the deposited thin films. Fig.2 shows the surface morphologies of the TiO_2 films. It shows that the glass substrate is entirely covered with spherically nanograined TiO_2 particles. The influence of low deposition temperature on the formation of TiO_2 crystals could be easily noticed from the fact that the crystallites formed from the solution at low deposition rates had well defined multi grain agglomerates possessing irregular shape and size. In addition, the formation of semi-spherical TiO_2 particles was observed with increasing deposition time. This clearly indicates the influence of deposition time and the fact that the growth of TiO_2 microspheres was initially suppressed by premature termination of the growth process, but irregular

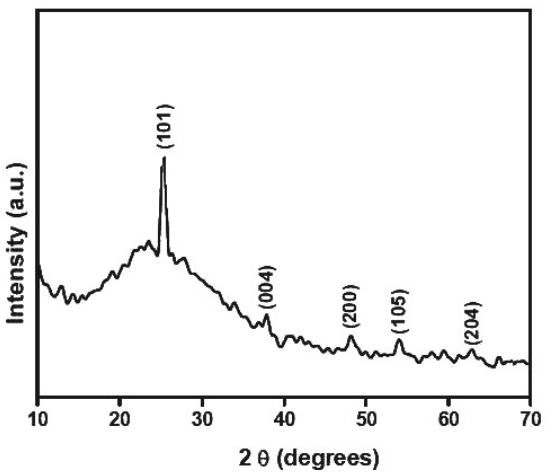

Fig.1. The XRD pattern of the TiO_2 thin film

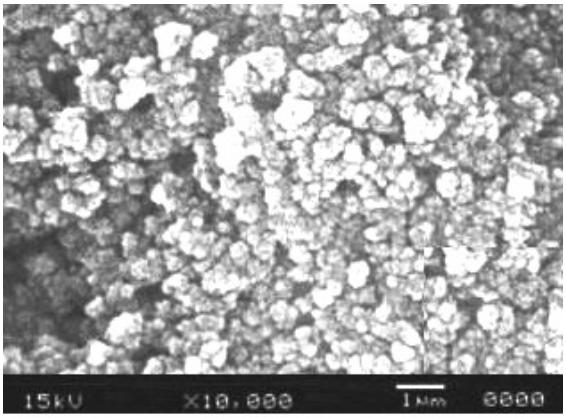

Fig.2 SEM image of the TiO_2 thin film

shaped particles were transformed to semi-spherical particles as the deposition time increased corroborates the indication. Nevertheless, many cracks developed on relatively thick films despite the increase in film thickness with increase in the deposition time.

4.3 Optical properties

The optical properties of TiO_2 films were studied using the absorption spectrum recorded with the help of a UV-Vis spectrophotometer. The optical absorption spectrum of the TiO_2 films was recorded in the range of 300-800 nm. The absorption spectrum of TiO_2 thin films is shown in Fig.3 (a). A significant decrease in the wavelength can be ascribed to the absorption of light caused by the excitation of electrons from the valence band to the conduction band of titania [18]. It was observed that the optical absorption decreased smoothly from the UV to near IR region. The optical absorption coefficient (α) was calculated from transmittance using the following relation

$$\alpha = \frac{1}{d}\log\left(\frac{1}{T}\right) \tag{2}$$

where T is the transmittance and d is the thickness of the film. As a direct band gap material, the film under study has an absorption coefficient (α) obeying the following relation for high photon energies (hν)

$$\alpha = \frac{A\left(h\nu - E_g\right)^{1/2}}{h\nu} \tag{3}$$

where E_g is the band gap of the TiO_2 films and A is a constant. A plot of variation of $(\alpha h\nu)^2$ versus hν is shown in Fig.3(b). E_g was evaluated using the extrapolation of the linear part. Using Tauc's plot, the energy gap (E_g) was calculated to be 3.6 eV.

4.3.1 Determination of Optical Constants

Two of the most important optical properties, namely the refractive index and the extinction coefficient are generally called optical constants. The amount of light that transmits through thin film material depends on the amount of the reflection and the absorption that take place along the light path. The absorption of radiation that leads to electronic transitions between the valence and conduction bands is split into direct and indirect transitions. The optical constants such as refractive index, extinction coefficient and electric susceptibility were then calculated using the relation given below: The extinction coefficient (K) could be obtained from the following equation

$$K = \frac{\lambda\alpha}{4\pi} \tag{4}$$

The extinction coefficient (K) was found to be 0.0030 at λ =800 nm. The transmittance (T) is given by

$$T = \frac{(1-R)^2\exp(-\alpha t)}{1-R^2\exp(-2\alpha t)} \tag{5}$$

Reflectance (R) in terms of absorption coefficient could be obtained from the above equation.

Hence we have

$$R = \frac{1 \pm \sqrt{1-\exp(-\alpha t + \exp(\alpha t)}}{1+\exp(-\alpha t)} \tag{6}$$

Refractive index (n) can be determined from the reflectance data using the following equation

$$n = -\frac{(R+1) \pm \sqrt{3R^2+10R-3}}{2(R-1)} \tag{7}$$

The refractive index (n) was found to be 1.65 at λ =800 nm. This result revealed that TiO_2 film has high refractive index. The high refractive index of TiO_2 films makes it suitable for use as anti-reflection coatings. From the optical constants, electric susceptibility (χ_c) could be calculated according to the following relation

$$\varepsilon_r = \varepsilon_0 + 4\pi\chi_C = n^2 - k^2 \tag{8}$$

Hence we have

$$\chi_C = \frac{n^2 - k^2 - \varepsilon_0}{4\pi} \tag{9}$$

where ε_0 is the permittivity of free space and k is extinction coefficient. The value of electric susceptibility (χ_c) was 1.723 at λ=800 nm. Since electrical susceptibility is greater than 1, the material can be easily polarized when the incident light is more intense. The optical behaviour of the films can be correlated with dielectric behaviour. The complex dielectric constant is a fundamental intrinsic material property. The real part of it accounts for how much it will slow down the speed of light in the material and the imaginary part explains how a dielectric absorbs energy from the electric field due to dipole motion.The real part dielectric constant (ε_r) and the imaginary part dielectric constant (ε_i) could be calculated from the following relations:

$$\varepsilon_r = n^2 - k^2 \tag{10}$$

$$\varepsilon_i = 2nk \tag{11}$$

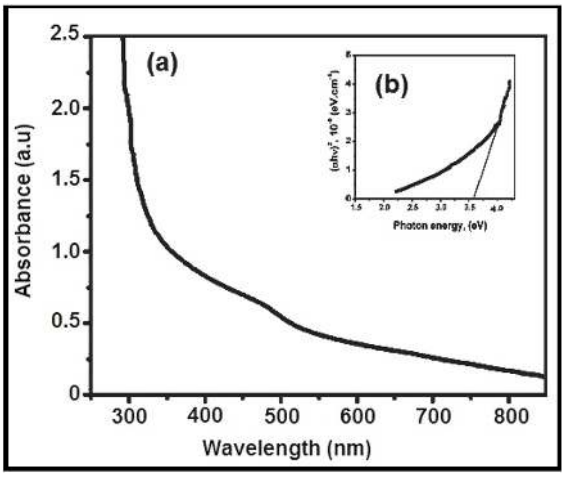

Fig.3 (a) The optical absorbance spectrum of TiO_2 thin film (b) Plot of $(\alpha h\nu)^2$ Vs (hν)

The values of the real dielectric constant (ε_r) and the imaginary dielectric constant (ε_i) at λ=800 nm were estimated to be 3.735 and 0.0425 respectively. The lower and positive value of dielectric constant of the material enables the occurrence of the induced polarization due to intense incident light radiation. Titanium dioxide (TiO_2) has attracted significant attention from researchers because of its many interesting physical and chemical properties that make it suitable for a variety of applications. For instance, TiO_2 has high corrosion resistance and chemical stability and an excellent optical transparency in the visible and near infrared regions. It also has high refractive index that makes it suitable for anti-reflection coatings in optical devices. It has been used mostly as a pigment in paints, sunscreens, ointments, toothpaste etc.

4.5 PL studies

The photoluminescence spectrum (PL) of the TiO_2 films was recorded in the range of 375-550 nm with an excitation wavelength of 300 nm. Fig.4 shows the PL spectrum of the TiO_2 thin films. The peak present at 387 nm corresponds to the band-to-band transition due to excitation of electrons from valence band to conduction band. The calculated band gap using this peak was 3.60 eV, which corresponded to the band gap of anatase phase of TiO_2 thin films. The presence of broader photoluminescence band in the visible green region could be attributed to the recombination of photo-generated holes with the singly ionized oxygen vacancies. There is a weak broad band in the visible region. The bluish-green and yellow-green emissions are attributed to deep level defects in TiO_2 films, such as doubly-ionized and single-ionized interstitial Ti vacancies and oxygen vacancies [21]. The main peaks are located at about 387 nm. In the nanocrystalline regime, since the number of molecules at the surface is more, surface defects play a very important role in determining the luminescence characteristics.

4.6 FTIR Analysis

Fourier Transform Infrared (FTIR) spectroscopy is a potential method for observing molecular vibrations. The FTIR spectrum of the TiO_2 thin films are shown in Fig.5. From this spectrum, it is observed that strong band around at 620 cm^{-1} is associated with the characteristic vibrational mode of anatase TiO_2. The absorption peak at around 900 cm^{-1} is assigned to characteristic stretching vibration of peroxo groups. The absorption peaks around 1370 and 1638 cm^{-1} may be due to the stretching and bending vibration of hydroxyl groups of molecular water. The narrow band around 2923 cm^{-1} is due to organic residues [22]. The absorption at 3391 cm^{-1} indicates the presence of hydroxyl group [23]. As-deposited TiO_2 showed the higher depth at 3391cm^{-1}.Thus the results indicate the presence of Ti-O bonds, peroxo groups and OH groups for as-deposited film.

4.7 Dielectric Properties

The variations of the dielectric constant and the dielectric loss of the TiO_2 thin film at frequencies from 50Hz to 5 MHz and at different temperatures are displayed in Figs. 6 and 7. The dielectric constant could be calculated using the formula

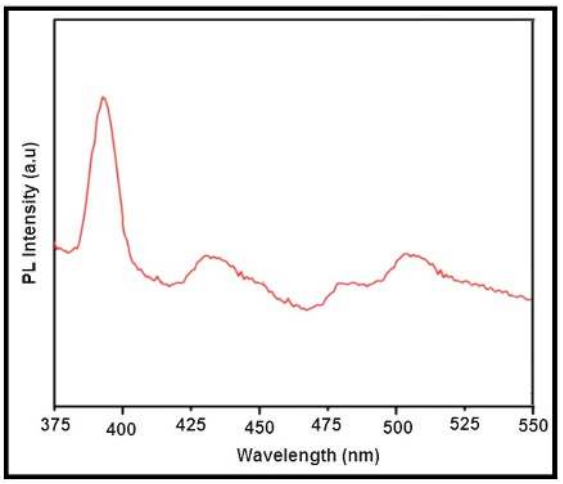

Fig.4. Photoluminescence spectrum of the TiO_2 thin films

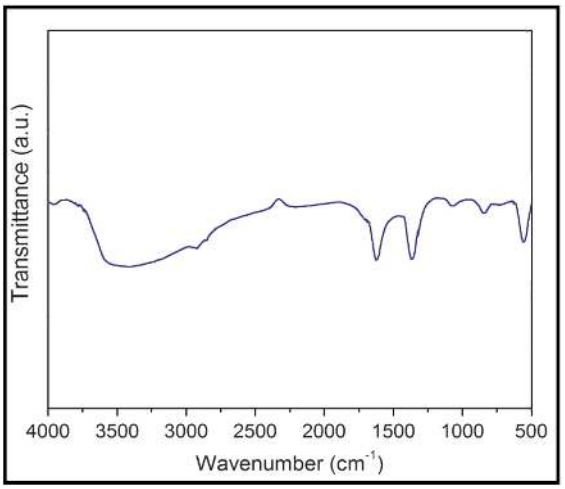

Fig.5. FT-IR spectrum of TiO_2 thin film

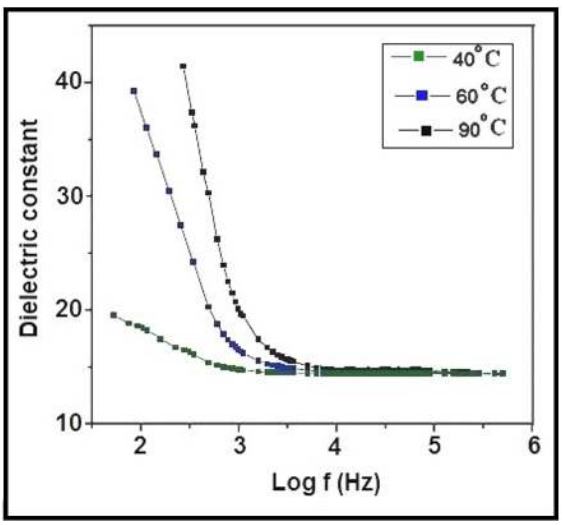

Fig.6. Dielectric constant of TiO_2 thin film

$$\varepsilon_r = \frac{Cd}{\varepsilon_0 A} \quad (12)$$

ε_r is used to evaluate the dielectric constant , where *d* is the thickness of film and *A* is the area of the film. Fig.6 shows the plots of dielectric constant against log frequency. It was observed that the dielectric constant decreased exponentially with increasing frequency and then attained almost a constant value in the high frequency region. This also indicated that the value of the dielectric constant increased with an increase in the temperatures. The net polarization present in the material is due to ionic polarization, electronic polarization, dipolar polarization and space charge polarization[24]. The contribution of the decrease in the dielectric constant due to electronic polarization is quite less [25]. Dipolar polarization is also expected to decrease with temperature as it is inversely proportional to temperature. The contribution to polarizability of the space charge depends on the purity of the nanoparticles[26]. At low temperature and high frequency, we may take it as negligible. However, it is significant in the low frequency region. As the temperature increases, the contribution of the space charge effect towards polarization may have a tendency to increase [27]. Fig.7 shows the variation of the dielectric loss with respect to the frequency at different temperatures. It was observed that the dielectric loss showed a decreasing trend with increasing frequency. These curves suggest that the dielectric loss is strongly dependent on the frequency of the applied field, similar to that of the dielectric constant. In the low frequency region, high energy loss is observed, which may be due to the dielectric polarization, space charge and rotation direction polarization occurring in the low frequency range. The high values of dielectric loss at low frequencies could be related to the charge lattice defect of the space charge polarization [28].

4.8 AC electrical conductivity studies

The ac conductivity (σ_{ac}) was calculated for the TiO_2 thin films from the following formula

$$\sigma_{ac} = \varepsilon_0 \varepsilon_r \omega \tan\delta \quad (13)$$

where ε_o is the vacuum dielectric constant (8.85×10^{-12} farad/m), tanδ is the dielectric loss, ε_r is the relative dielectric constant, and ω is the angular frequency $\omega = 2\pi\nu$ of the applied field. Fig.8 shows the variation of ac conductivity with various frequencies and temperatures. It was observed that the value of ac conductivity increased with increase in frequency. The activation energy required for the conduction process of the charge carriers as well as the activation energy of the TiO_2 thin films was found to be 0.72 eV. The conduction mechanism can be explained by the rotation of ions when the temperature of the material is increased. The rotation of ions causes local displacement of electrons in the direction of the applied field, which in turn leads to increase in induced polarization [29].

4.6 Photoconductivity Studies

The photo current and the dark current were plotted as a function of the applied field and the same is shown in Fig.9. The plots indicate a linear increase of current in the dark and the visible light illuminated TiO_2 thin films in

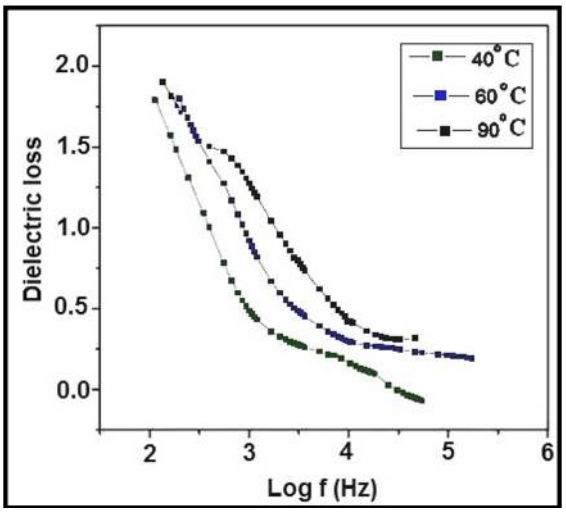

Fig.7. Dielectric loss of TiO_2 thin film

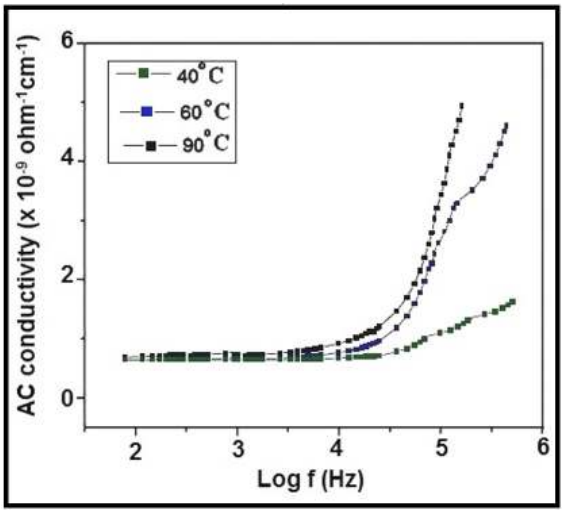

Fig.8. Variation of conductivity with log frequency

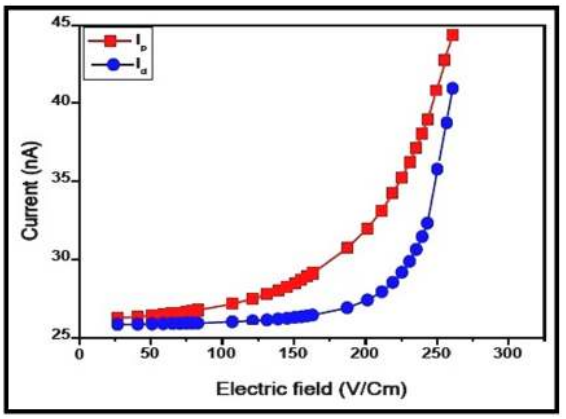

Fig.9. Photoconductivity study of TiO_2 thin films

cases with an increase in applied field depicting the ohmic nature of the contacts [30]. It was observed that both the dark and the photo currents increased linearly with the applied electric field with the dark current being less than the photocurrent which is termed positive photoconductivity. The low values of the dark current and insignificant rise in the photocurrent upon the visible light illumination were as expected. But the photocurrent was found to be more than the dark current. Hence, it could be said that the TiO_2 thin films exhibited positive photo conductivity. This was caused by the generation of mobile charge carriers which in turn were caused by the absorption of photons. This was because of an increase in the number of charge carriers or their life time in the presence of radiation [31] . The positive photoconductivity of the films might be due to the increase in the number of charge carriers to reveal the conducting nature of the material. The dark current was less than the photocurrent, signifying positive photoconductivity nature confirmed by the reported results [32].

5. CONCLUSION

Recently, titanium oxide (TiO_2) thin films have emerged as one of the most promising oxide materials owing to their optical, electrical and photo electrochemical properties. In this study, TiO_2 thin film was deposited on glass substrate using chemical bath deposition (CBD) technique. The structural and morphological properties of TiO_2 thin films were investigated by XRD and SEM methods. The UV-Visible and Photoluminescence spectrum showed excellent transmission in the entire visible region. The optical properties such as band gap, refractive index, extinction coefficient and electrical susceptibility were calculated to analyze the optical property. The FT-IR spectrum confirmed the strong presence of TiO_2. The dielectric constant and the dielectric loss of the TiO_2 thin films were measured for different frequencies and temperatures. AC electrical conductivity was found to increase with an increase in the temperature and frequency. The activation energy was found to be 0.72 eV. The photoconductivity study ascertained the positive photoconductivity nature of the TiO_2 thin films. A wide range of these materials is now available and in use in many commercial, industrial and military applications. Similarly, when TiO_2 is reduced to nanoscale, it shows unique properties, of which the electrical aspect is of paramount importance. Some of the current research and development works are in the area of these nanomaterials. This speaks of the possibilities of applications in which material nanostructures can be used to produce optical and electronic properties.

REFERENCES

1. Maurice V, Georgelin T, Siaugue JM, Cabuil V. Synthesis and characterization of functionalized core-shell gamma Fe2O3-SiO2 nanoparticles. *Journal of Magnetism and Magnetic Materials*. 2009;321(10):1408–1413. doi:10.1016/j.jmmm.2009.02.051
2. Bala H, Zhang Y, Ynag H, Wang C, Li M, Lv X, Wang Z. Preparation and characteristics of calcium carbonate/silica nanoparticles with core-shell structure. *Colloids and Surfaces A*. 2007;294(1):8–13. doi:10.1016/j.colsurfa.2006.07.051
3. Okada M, Yamada Y, Jin P, Tazawa M, Yoshimura K. Fabrication of multifunctional coating which combines low-e property and visible-light-responsive photocatalytic activity. *Thin Solid Films*. 2003;442(1):217-221. doi:10.1016/S0040-6090(03)00985-4
4. Ennaoui A, Sankapal BR, Skryshevsky V, Lux-Steiner MC. TiO2 and TiO2-SiO2 thin films and powders by one-step soft-solution method: Synthesis and characterizations. *Solar Energy Materials and Solar Cells*. 2006*;90*(10):1533-1541. doi:10.1016/j.solmat.2005.10.019
5. Weinberger R, Garber RB. Titanium-dioxide photocatalysts produced by reactive magnetrón sputtering. *Applied Physics Letters*. 1995;66(18):2409-2411.
6. Manno D, Micocci G, Rella R, Serra A, Taurino A, Tepore A. Titanium oxide thin films for NH_3 monitoring: Structural and physical characterizations. *Journal of Applied Physics*. 1997;82(1):54-59. http://dx.doi.org.ez69.periodicos.capes.gov.br/10.1063/1.365848
7. Wang Z, Hu X. Fabrication and electrochromic properties of spin-coated TiO2 thin films from peroxo-polytitanic acid. *Thin Solid Films*. 1999;352:62-65. doi:10.1016/S0040-6090(99)00321-1
8. Ramadoss A, Kim SJ. Vertically aligned TiO 2 nanorod arrays for electrochemical supercapacitor. *Journal of Alloys Compounds*. 2013;561:262-267.
9. Ambade SB, Ambade RB, Mane RS, Lee GW, Shaikh SF, Patil SA. Low temperature chemically synthesized rutile TiO2 photoanodes with high electron lifetime for organic dye-sensitized solar cells. *Chemical Communications*. 2013;49(28):2921-2923.
10. Yin X, Que W, Fei D, Xie H, He Z. Effect of TiO2 shell layer prepared by wet-chemical method on the photovoltaic performance of ZnO nanowires arrays-based quantum dot sensitized solar cells. *Electrochimica Acta.* 2013;99:204-210. doi:10.1016/j.electacta.2013.03.110
11. Han B, Kim SJ, Hwang BM, Kim SB, Park KW. Single-crystalline rutile TiO2 nanowires for improved lithium ion intercalation properties. *Journal of Power Sources*. 2013;222:225-229. doi:10.1016/j.jpowsour.2012.08.073
12. Nakata K, Fujishima A. TiO2 photocatalysis: Design and applications. *Journal of Photochemistry and Photobiology C: Photochemistry Reviews.* 2012;13(3):169-189. doi:10.1016/j.jphotochemrev.2012.06.001
13. Fabrega C, Andreu T, Tarancon A, Flox C, Morata A, Barrio LC, et al. Optimization of surface change transfer processes on rutile TiO2 nanorods photoanodes for water splitting. *International Journal of Hydrogen Energy*. 2013;38:2979.
14. Ding SN, Gao BH, Shan D, Suna YM, Cosnier S. TiO2 nanocrystals electrochemiluminescence quenching by biological enlarged nanogold particles and its application for biosensing. *Biosensors & Bioelectronics*. 2013;39(1):342-345. DOI: 10.1016/j.bios.2012.07.065
15. Tobaldi M, Pullar RC, Gualtieri AF, Seabra MP, Labrincha JA. Phase composition, crystal structure and microstructure of silver and tungsten doped TiO2nanopowders with tuneable photochromic behaviour. *Acta Materialia.* 2013;61(15):5571-5585. doi:10.1016/j.actamat.2013.05.041
16. Hebeish A, Abdelhady MM, Youssef AM. TiO2 nanowire and TiO2 nanowire doped Ag-PVP nanocomposite for antimicrobial and self-cleaning cotton textile. *Carbohydrate Polymers*. 2013;91(2):549-559. doi:10.1016/j.carbpol.2012.08.068
17. Herzog C, Belaidi A, Ogachoa A, Dittrich T. Inorganic solid state solar cell with ultra-thin nanocomposite absorber based

on nanoporous TiO2 and In2S3. *Energy Enviromental Science.* 2009;2:962-964. DOI: 10.1039/B906273D

18. Liu JX, Yang DZ, Shi F, Cai YJ. Sol– gel deposited TiO film on NiTi surgical alloy for biocompatibility improvement'. *Thin Solid Films*. 2003;429:225-230.
19. ElFanaoui A, Boulkaddat L, Taleb A, Ihlal A, ElHamri E, Meddah M, et al. Solid Inorganic Compounds - Characterisation of TiO2 thin films prepared by chemical bath deposition. *Annales de Chimie Science des Matériaux.* 2011;36(1):37.
20. Mayabadi AH, Waman VS, Kamble MM, Ghosh SS, Gabhale BB, Rondiya SR, et al. Evolution of structural and optical properties of rutile TiO2thin films synthesized at room temperature by chemical bath deposition method. *Journal of Physics and Chemistry of Solids*. 2014;75(2):182–187.doi:10.1016/j.jpcs.2013.09.008
21. Senthil TS, Muthukumarasamy N, Velauthapillai D, Agilan S, Thambidurai M, Balasundaraprabhu R. Natural dye (cyanidin 3-O-glucoside) sensitized nanocrystalline TiO2 solar cell fabricated using liquid electrolyte/quasi-solid-state polymer electrolyte. *Renewable Energy*. 2011;36(9):2484-2488 doi:10.1016/j.renene.2011.01.031
22. Maira AJ, Coronado JM, Augugliaro V, Yeung KL, Conesa JC, Soria J. Fourier transform infrared study of the performance of nanostructured TiO 2 particles for the photocatalytic oxidation of gaseous toluene. *Journal of Catalysis.* 2001;202(2):413. doi:10.1006/jcat.2001.3301
23. Karuppuchamy S, Jeong JM. Synthesis of nano-particles of TiO2 by simple aqueous route. *Journal Oleo Science*. 2006;55:263-266.
24. Suresh S. Wet chemical synthesis of tin sulfide nanoparticles and its characterization. *International Journal of Physical Sciences*. 2014;9(17):380-385.
25. Suresh S. Synthesis, structural and dielectric properties of zinc sulfide nanoparticles. *International Journal of Physical Sciences*. 2013;8(21):1121-1127.
26. Suresh S. Synthesis and electrical properties of TiO2 nanoparticles using a wet chemical technique. *American Journal of Nanoscience and Nanotechnology*. 2013;1(1):27-30.
27. Suresh S, Arunseshan C. Dielectric Properties of Cadmium Selenide (CdSe) Nanoparticles synthesized by solvothermal method. *Appllied Nanoscience*. 2014;4(2):179–184.
28. Suresh S. Studies on the dielectric properties of CdS nanoparticles. *Appllied Nanoscience*. 2014;4(3):325–329.
29. Thirumavalavan S, Mani K, Suresh S. Investigation on structural, optical, morphological and electrical properties of lead sulphide (PbS) thin films. *Journal of Ovonic Research*. 2015;11:123 – 130.
30. Bube RH. *Photoconductivity of solids*. New York: Wiley Interscience; 1981.
31. Thirumavalavan S, Mani K, Suresh S. Structural, surface morphology, optical and electrical investigation of cdse thin films. *Chalcogenide Letters.* 2015;12:237-246.
32. Thirumavalavan S, Mani K, Suresh S. Investigations on the photoconductivity studies of ZnSe, ZnS and PbS thin films. *Scientific Research and Essays.* 2015;10:378-382.